

Simulation of damage around a circular opening in rock

A. Golshani, Y. Okui, M. Oda

Dept. of Civil Engineering, Saitama University, Saitama, Japan

K. Suzuki

Geotechnical Eng. Dept., Technical Research Institute, Obayashi Corporation, Tokyo, Japan

Keywords: creep, evolution damage zone, underground opening, numerical simulation

ABSTRACT: The time-dependent mechanical and hydraulic behaviour of rock in the excavation disturbed zone (EDZ) in the vicinity of underground facilities is important for the safety assessment of these underground excavations. To simulate the evolution disturbed zone (EDZ) around a circular opening in granitic rocks under creep test (biaxial), a micromechanics-based continuum damage model (Golshani et al., 2003) is used. Then, the numerical results are compared to the experimental data from the creep test on a rectangular prism specimen of Inada granite containing a circular opening. The results of numerical simulation are in good agreement with the experimental test and indicate that the damage evolution zone mainly occurs in the side walls of the opening under biaxial creep condition.

1 Introduction

The excavation of underground openings results in a change in stress distribution and pore water pressure leading to the development of fractures. Such changes alter the mechanical rock mass properties such as strength and deformability, and the hydraulic conductivities and hence influence contaminant pathways.

Depending on mechanical host rock properties, the stress redistribution may lead to the development of a plastic zone around the tunnel, termed as excavation disturbed zone (EDZ). One of the major problems in the assessment of safety of underground facilities such as waste disposal storage is the transmissivity of the EDZ zone. In other words, the EDZ with its increased permeability constitutes a potential risk to the effectiveness of the storage in waste isolation from the accessible environment.

The failure mechanism in the EDZ zone is the initiation and growth of microcracks. To characterize the behavior of the EDZ zone, time influence on the mechanical properties of rock is of great importance. Under constant loading (creep), the microcracking occurs through two mechanisms: stress-induced microcrack growth and time dependent microcrack growth. Time dependent failure of brittle rocks under constant loading results from stable microcracks growth. This stable microcrack growth, called sub-critical crack growth, can occur even if the stress intensity factor at microcrack tip is below fracture toughness.

Analytical and numerical solution for modeling of the EDZ in the vicinity of underground excavations exists (e.g. Souley et al., 2001; Fakhimi et al., 2002; Chen et al., 2004), however, there is very little knowledge on the actual development of the EDZ starting from microcracking of intact rock around the openings under creep loading.

By drawing on this background information, this paper utilizes the micromechanics-based continuum damage model proposed by Golshani et al. (2004) to simulate the EDZ and its time-dependent development. Furthermore, numerical data will be compared to the results of a plane stress (biaxial) creep test which was performed on a rectangular sample containing a circular opening of Inada granite (from a quarry in Kasama, Ibaraki, Japan).

2 A brief review of damage model

In this model, a rock is idealized as an elastic material with N groups of microcracks. Each microcrack group is characterized by its unit vector $n^{(i)}$, the average microcrack length $2c^{(i)}$ and the number $\rho^{(i)}$ of microcracks per unit area of material in group i (Number density of microcracks). It is assumed that the matrix material remains elastic during the entire loading history and all inelastic deformation is due to microcracking (brittle materials). Therefore, the stress-strain relationship is given by (e.g. Horii and Nemat-Naseer, 1983):

$$\sigma = D_e : (\varepsilon_t - \varepsilon^*) \quad (1)$$

where D_e is the elastic modulus tensor, ε_t is total strain and ε^* is inelastic strain associated with the opening of microcracks. For each group of microcracks, the inelastic strain is as a function of the number density of microcracks, microcracks length, microcracks orientation: $\theta^{(i)}$ and the applied stress. Therefore, the total inelastic strain is given by (see for more detail, Golshani et al, 2004):

$$\varepsilon^* = \sum_{i=1}^N \varepsilon^*(\rho^{(i)}, c^{(i)}, \theta^{(i)}, \sigma) \quad (2)$$

By assuming that microcrack growth occurs in tensile mode, the stress intensity factor K_I for a single microcrack with length of $2c$ and the orientation angle of θ is approximated by

$$K_I = \sqrt{\pi c \sigma'_t} \quad (3)$$

where σ'_t is the local tensile stress acting normal to the microcrack surface (Fig. 1), which is generated as a result of sliding up on asperities and is expressed by (with respect to local coordinate):

$$\sigma'_t = \sigma'_{22} + f(c)S'_{22} \quad (4)$$

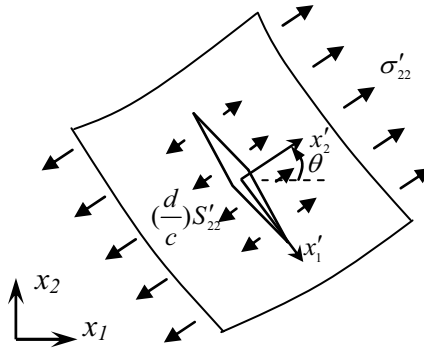


Figure 1. Microcrack under local tensile stress

The first term on the right hand side of Eq. (4) is the normal stress acting on the microcrack surface, which arises from the far field compressive stress and inhibits microcrack growth. The second term is the tensile stress reflecting the effect of asperities, which is assumed to be proportional to the

deviatoric stress S'_{22} and $f(c)$ is a proportionality coefficient depending on only c . It should be mentioned that microcrack growth causes the tensile stress to be relieved as the microcrack propagate. Otherwise, microcrack would propagate without any limit. Therefore, it is assumed that the $f(c)$ is inversely proportional to the half of microcrack length;

$$f(c) = d / c \quad (5)$$

Here d is a typical length scale of material such as grain size. The microcrack growth law for stress-dependent propagation is given as follows:

$$K_I - K_{IC} = 0 \quad (6)$$

In this case, microcrack grows because the stress in the region surrounding the microcrack is sufficient to cause the stress intensity factor: K_I to equal the fracture toughness: K_{IC} .

On the other hand, for time-dependent microcrack growth the subcritical microcrack growth rate dc / dt is assumed to obey a power law (Atkinson, 1984):

$$dc / dt = A(K_I / K_{IC})^n \quad (7)$$

where A and n are sub-critical microcrack growth parameters which depend on the type of rock and environmental conditions.

In deformation and failure of brittle materials, isolated microcrack growth occurs only at relatively low stresses. Once numerous microcracks begin to grow, interaction among them starts to play a very important role in the evolution of further microcracking. Eq. (4) was formulated by disregarding the existence of neighboring open microcracks, so that its use should be limited within the early stage of non-elastic deformation where interaction among open microcracks is not dominant. The so-called pseudo-traction method provides a powerful tool for evaluating the elastic interaction among microcracks (Horii and Nemat-Nasser, 1985a, b). To outline the principle, we first consider an infinite plate with two open (not potential) microcracks α and β of lengths $2c_\alpha$ and $2c_\beta$, respectively, which is subjected to far field stresses (Fig. 2). Two coordinate systems, $x_i'^\alpha$ and $x_i'^\beta$ ($i=1, 2$), are employed such that their origins, o_α and o_β , are located at the centers of the open microcracks α and β . Note that the axes $x_2'^\alpha$ and $x_2'^\beta$ are taken to be normal to the open microcrack surfaces. The symbols in Fig. 2 are defined as follows:

$d_{\alpha\beta}$ = distance between the origins of the two open microcracks α and β ,

$\theta_{\beta\alpha}$ = inclination angle of $x_2'^\alpha$ to $x_2'^\beta$, and

$\phi_{\beta\alpha}$ = angle between the axis $x_1'^\alpha$ and the $o_\alpha o_\beta$ direction.

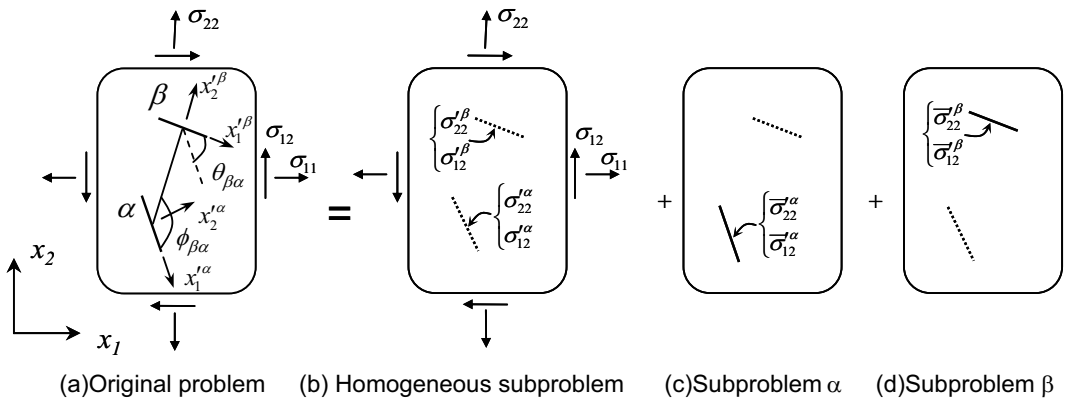


Figure 2. Decomposition of an original problem

Our original boundary problem is decomposed into three sub-problems; i.e., one homogenous sub-problem and two sub-problems α and β (Fig. 2). In the homogenous sub-problem, there is no open microcrack and the domain is subjected to the same far field stresses, σ_{11} , σ_{22} and σ_{12} , as those in the original problem. In sub-problem α , one open microcrack α is considered in the infinite solid under zero far field stresses. The stresses $\bar{\sigma}'_{22}{}^{\alpha}$ and $\bar{\sigma}'_{12}{}^{\alpha}$ are applied, as boundary stresses, on the surface of open microcrack α . Similarly, the boundary stresses $\bar{\sigma}'_{22}{}^{\beta}$ and $\bar{\sigma}'_{12}{}^{\beta}$ are also applied on the surface of open microcrack β in sub-problem β .

The stresses must be zero on the surface of the *open* microcrack α in the original boundary problem. This requirement is satisfied by means of the following equalities:

$$\bar{\sigma}'_{22}{}^{\alpha} + \sigma'_{22}{}^{\alpha} + \sigma'^{P\alpha}_{22} = 0 \quad (8a)$$

$$\bar{\sigma}'_{12}{}^{\alpha} + \sigma'_{12}{}^{\alpha} + \sigma'^{P\alpha}_{12} = 0 \quad (8b)$$

where $\sigma'_{22}{}^{\alpha}$ and $\sigma'_{12}{}^{\alpha}$ are the stresses at the position of microcrack α arising from the far field stress in the homogenous sub-problem, and the quantities $\sigma'^{P\alpha}_{22}$ and $\sigma'^{P\alpha}_{12}$, called the pseudo-tractions, are the stresses at the position of microcrack α in sub-problem β .

The pseudo-tractions must be determined such that all the boundary conditions for the original problem are satisfied. Using Muskhelishvili's complex stress function, we can obtain an equation called the consistency equation to ensure the traction-free condition on the surface of the open microcrack, as follows (see Okui et al., 1993):

$$\{\sigma'^{P\alpha}\} = [\gamma'^{\alpha\beta}] (\{\sigma'^{\beta}\} + \{\sigma'^{P\beta}\}) \quad (9)$$

where $\{\sigma'^{P\alpha}\} = \{\sigma'^{P\alpha}_{11}, \sigma'^{P\alpha}_{22}, \sigma'^{P\alpha}_{12}\}^T$, $\{\sigma'^{\beta}\} = \{\sigma'^{\beta}_{11}, \sigma'^{\beta}_{22}, \sigma'^{\beta}_{12}\}^T$, and $\gamma'^{\alpha\beta}$ is a 3 by 3 matrix whose elements are functions of the position vectors at the center of microcracks, angle between microcracks surfaces $\theta_{\alpha\beta}$, length of the source microcrack and d . In Eq. (9) only two microcracks are considered. In reality, however, a huge number of microcracks are distributed in the domain and the consistency equation: Eq. (9) can be generalized as an integral equation for all microcracks. Considering the effect of interaction, the stress intensity factor equation can be rewritten as follows:

$$K_I(\sigma, \sigma^P, c) = \sqrt{\pi} c \left[(\sigma_{11} + \sigma_{11}^P) + f(c) \left(\frac{(\sigma_{11} + \sigma_{11}^P) - (\sigma_{22} + \sigma_{22}^P)}{2} \right) \right] \quad (10)$$

Finally, the governing equations are stress-strain relationship: Eq. (1), stress-dependent microcrack growth law: Eq. (6), time-dependent microcrack growth law: Eq. (7) and consistency equation: Eq. (9). All the parameters of this model can be determined from triaxial compression tests and observation of microcracks growth under microscope.

3 Analysis of a rectangular sample containing an opening

Finite element method was used to solve the governing equations of the damage model described above on a numerical basis. Because our intension was to simulate the EDZ in the vicinity of the underground openings and its time-dependent development, a rectangular sample (500 mm*500 mm) containing a 160 mm diameter circular hole was chosen (Fig. 3a). The finite element mesh is shown in Fig. 3b. The number of elements and nodes are 290 and 168 and a plane stress condition (biaxial loading) was considered in the analysis. For simplicity, pre-existing microcracks were classified into two groups, depending on their orientations; i.e., vertical and horizontal and for each set of microcracks, the initial mean length: $2c_0$ and initial number density: ρ were calculated through

observation under microscope. All parameters that appeared in the governing equations for Inada granite are listed in Table 1.

In numerical simulations, a stress dependent analysis was performed until reaching the desired stress state and then a time dependent analysis was started. Note that confining pressure was $\sigma_{11} = 10$ MPa and creep stress held at $\sigma_{22} = 40$ MPa.

Table 1. Model parameters used in numerical simulation for time dependent behavior of Inada granite.

Parameter	Value(s)	
Young's modulus	$E = 73\text{GPa}$	
Poisson's ratio	$\nu = 0.23$	
Length parameter [mm]	$d = 0.34$	
Fracture toughness [$\text{MPa m}^{1/2}$]	$K_{IC} = 2.5$	
Microcracks orientation	Vertical	Horizontal
Initial microcrack length: $2c_0$ [mm]	1.12	1.08
Number density of microcracks: ρ [mm^{-2}]	0.45	0.67
Subcritical crack growth parameters	$n = 50 \quad A = 2.0\text{E-}23 \text{ m/s}$	

All data except subcritical crack growth parameters (Golshani et al., 2004) were reported by Golshani et al. (2003).

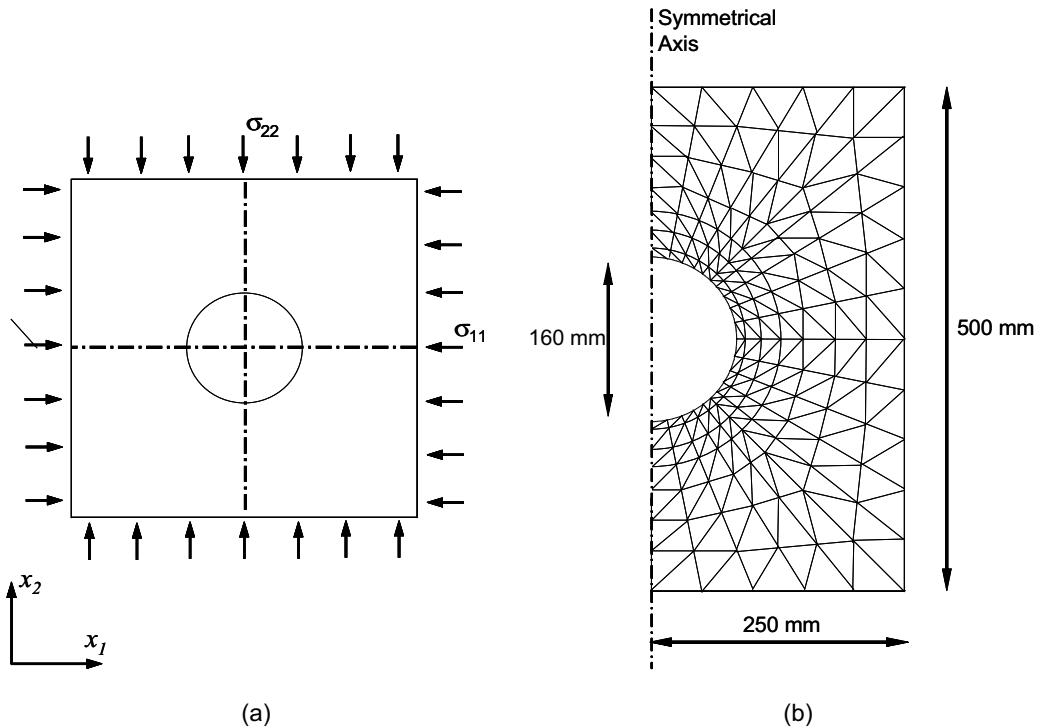


Figure 3. (a) A rectangular sample containing a circular opening (b) Finite element mesh

3.1 Results

In Fig. 4 microcracks length distribution at failure point is shown. Damage evolution zone which is caused by microcracking, in side wall area is larger than the roof and floor of the opening (e.g. Chen et al. 2004). Furthermore, increased compression occurs in the side wall area (Fig. 5). It can be concluded that the regions of increased compressive stress around the opening are disturbed more (This feature has been indicated for stress-dependent damage case by Read and Chandler, 1999). Also, the damage zone is limited to less than one radius of the opening in the surrounding rock.

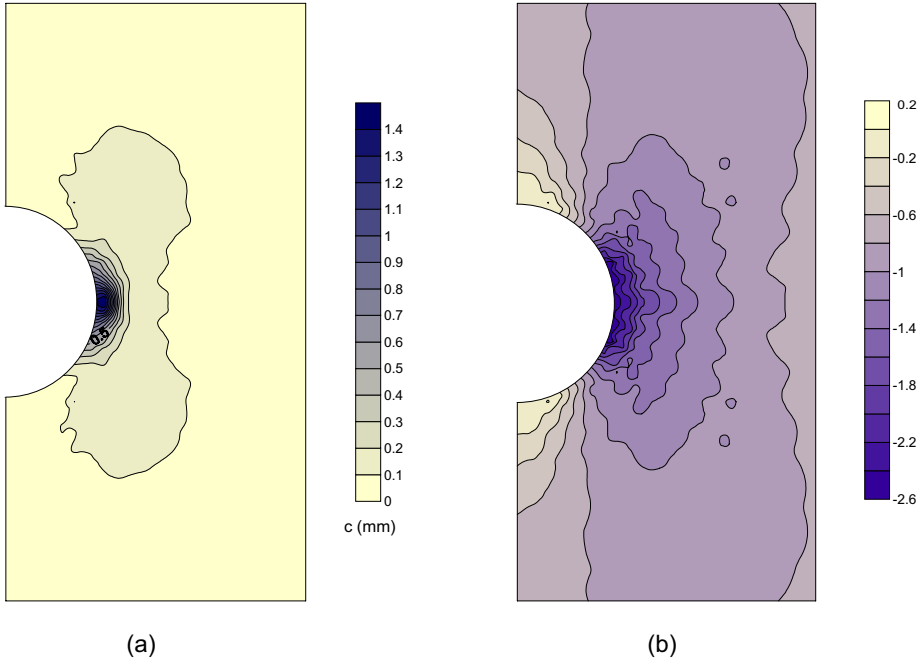


Figure 3. (a) Microcracks length distribution at failure (b) Normalized stress: σ_{11}/σ_0 distribution at failure (Note that σ_0 is the reference stress and is set to 63 MPa).

4 Experimental model

Creep test (biaxial, plane stress condition) was carried out using a rectangular prism of Inada granite containing a 16 mm diameter circular hole was tested to model time-dependent behaviour of an underground opening experimentally (Fig. 4).

The horizontal and vertical loads were applied at a rate of 10 KN/m simultaneously. When the horizontal load reached the required desired value (confining pressure equal to 10 MPa), it was stopped, while the applied vertical load increased at a constant strain rate of 0.25 mm/min. The vertical load was applied until the required value (vertical stress equal to 40 MPa) was achieved. Then, both horizontal and vertical loads were kept constant to simulate the constant stress state.

Acoustic emission (AE) was used to monitor the failure process during the creep test. Eight sensors, four on each face of the specimen as shown in Fig.4, were used to monitor AE during the creep test.

Figures 5 and 6 show the location of the AE events which were recorded after 5521 seconds and 146755 seconds, respectively. It can be seen that the events were mainly concentrated around the side walls. Even though many events were recorded outside of the zone of one radius in the rock

mass around the opening, these events do not necessarily refer to the active microcracks which are significant in the sense of their effect on mechanical properties of rock mass such as the permeability.

5 Conclusions

The purpose of this study was to investigate numerically the damage evolution zone under creep condition around an opening in Inada granite. In this regard, a micromechanics-based continuum damage model proposed by Golshani et al. (2004) was used to simulate the evolution damage zone (EDZ) around an opening under creep condition. The results of numerical simulation are in good agreement with the experimental test. Both numerical modeling and experimental test indicate that the damage evolution zone mainly occurs in the side walls of the opening under biaxial creep condition. Also, from numerical simulation, it can be seen that the increased compression regions (around side walls) are mostly disturbed.

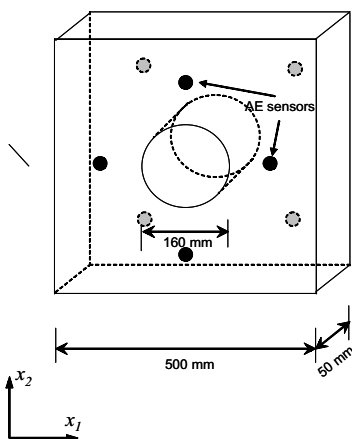


Figure 4. Specimen geometry and AE monitoring

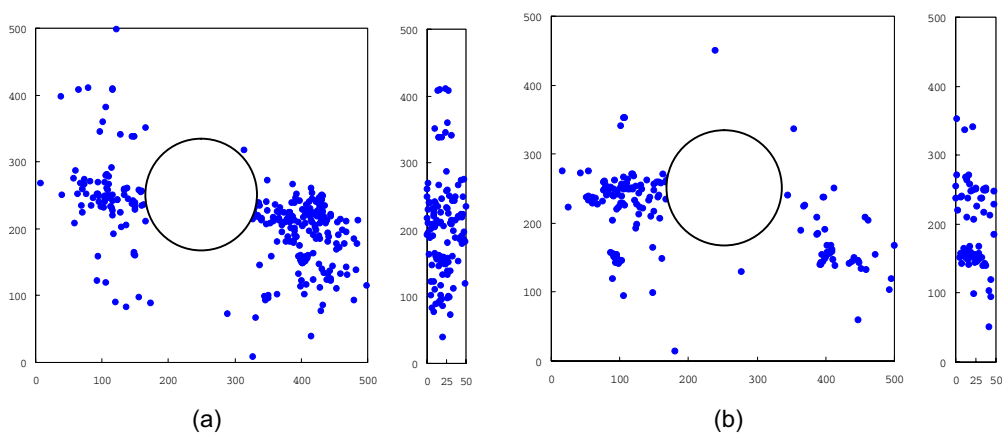


Figure 5. AE events location (filled circles): (a) after 5521 sec. (b) after 146755 sec.

6 Acknowledgements

This work was supported partially by Japan Society for the Promotion of Science (JSPS).

7 References

- Atkinson B.K. 1984. Subcritical crack growth in geological materials, *Journal of Geophysical Research*, 89(B6), 4077-4114.
- Chen W.Z., Zhu W.S., Shao J.F. 2004. Damage coupled time-dependent model of a jointed rock mass and application to large underground cavern excavation, *International Journal of Rock Mechanics and Mining Science*, 41, 669-677.
- Fakhimi A., Carvalho F., Ishida T., Labuz J.F. 2002. Simulation of failure around a circular opening in rock. *International Journal of Rock Mechanics and Mining Science*, 39, 507-515.
- Golshani A., Okui Y., Takemura T., Oda M.. 2004. Time dependent continuous damage model for brittle failure of rocks, *EUROCK 2004 & 53rd Geomechanics Colloquium*, Salzburg (Austria), 701-706.
- Golshani A. 2003, A micromechanical model for brittle failure of rock under compression, Ph.D. dissertation, Civil Engineering Department, Saitama University, Saitama (Japan), 80 pages.
- Horii H., Nemat-Nasser S. 1983. Overall moduli of solids with microcracks: load-induced anisotropy, *J. Mech. Phys. Solids*, 31(2), 155-177.
- Horii H., Nemat-Nasser S. 1985a. Compression-induced microcrack growth in brittle solids: axial splitting and shear failure, *Journal of Geophysical Research*, 90, 3105-3125.
- Horii H., Nemat-Nasser S. 1985b. Elastic fields of interacting inhomogeneities, *Int. J. Solids Struct.*, 21, 731-745.
- Hou Z. 2003. Mechanical and hydraulic behaviour of rock salt in the excavation disturbed zone around underground facilities, *International Journal of Rock Mechanics and Mining Science*, 40, 725-738.
- Okui Y., Horii H., Akiyama N. 1993. A continuum theory for solids containing micro defects, *Int. J. Rock Mech. Min. Sci. & Geomech. Abstr.*, 31(5), 735-749.
- Okui Y., Horii H. 1997. Stress and time-dependent failure of brittle rocks under compression: A theoretical prediction, *Journal of Geophysical Research*, 102 (B7), 14869-14881.
- Read R.S., Chandler N. 1999. Excavation damage and stability studies at the URL-rock mechanics considerations for nuclear fuel waste disposal in Canada, Proc. 37th US Rock Mechanics Symposium, Rotterdam, 2, 861-868.
- Souley M., Homand F., Pepa S., Hoxha D. 2001. Damage-induced permeability changes in granite: a case example at the URL in Canada, *International Journal of Rock Mechanics and Mining Science*, 38, 297-310.